



Quantum Chemical Calculation of 4-Amino-3-Nitrobenzonitrile for Dye Sensitized Solar Cells Applications

A. Prakasam	Department of Physics, Periyar University, Salem - 636 011, Tamil Nadu, India
P. Sakthivel	Department of Physics, Periyar University, Salem - 636 011, Tamil Nadu, India
P. M. Anbarasan	Centre for Nanoscience & Nanotechnology, Periyar University, Salem - 636 011, Tamil Nadu, India

ABSTRACT

The geometries, electronic structures, polarizabilities, and hyperpolarizabilities of organic dye sensitizer 4-Amino-3-Nitrobenzonitrile was studied based on *ab initio* HF and Density Functional Theory (DFT) using the hybrid functional B3LYP. Ultraviolet-visible (UV-Vis) spectrum was investigated by Time Dependent DFT (TDDFT). Features of the electronic absorption spectrum in the visible and near-UV regions were assigned based on TDDFT calculations. The absorption bands are assigned to $\pi \rightarrow \pi^*$ transitions. Calculated results suggest that the three excited states with the lowest excited energies in 4-Amino-3-Nitrobenzonitrile is due to photoinduced electron transfer processes. The interfacial electron transfer between semiconductor TiO₂ electrode and dye sensitizer 4-Amino-3-Nitrobenzonitrile, is due to an electron injection process from excited dye to the semiconductor's conduction band. The role of nitro group in 4-Amino-3-Nitrobenzonitrile in geometries, electronic structures, and spectral properties were analyzed.

KEYWORDS: Dye sensitizer, Density functional theory, Electronic structure, Absorption spectrum

1. Introduction

Because of the depletion of fossil fuels, growing demand of energy, global warming and other environmental problems, the development of environmental friendly renewable energy technologies is an urgent task for our human being [1]. Among all the renewable energy technologies, the nanocrystalline dye-sensitized solar cell (DSSC) system, a kind of photovoltaic device that presented by O'Regan and Gratzel in 1991, has attracted a lot of attention because of the potential application for low-cost solar electricity [2–5]. The main parts of DSSC are mesoporous oxide semiconductor layers that composed of nanoparticles and monolayer of dye sensitizers that attached to the surface of the semiconductor nano-films [3]. The dye sensitizers play an important role in DSSC that have a significant influence on the photoelectric conversion and transport performance of electrode [6–9]. Up to now, two kinds of dye sensitizers, which are generally known as metal-organic complexes and metal-free organic dyes, were studied extensively. In metal-organic complexes, especially the noble metal ruthenium polypyridyl complexes, including N3 and black dye etc. that were presented by Gratzel et al., have proved to be the best dye sensitizers with overall energy conversion efficiency greater than 10% under air mass (AM) 1.5 irradiation [10–12]. However, the limited metal Ru will become a bottleneck of application if the DSSC is widely used in our daily living [13]. On the other hand, metal-free organic dyes as sensitizers for DSSC, including cyanines, hemicyanines, triphenylmethanes, perylenes, coumarins, porphyrins, squaraines, indoline, and azulene- based dyes etc., have also been developed because of their high molar absorption coefficient, relatively simple synthesis procedure, various structures and lower cost [14–16]. In contrast to the numerous experimental studies of dye sensitizers, the theoretical investigations are relatively limited. Only several groups focused on the electronic structures and absorption properties of dye sensitizers [17–26], and Ru-complexes and organic dyes coupled TiO₂ nanocrystalline [27–30], as well as the electron transfer dynamics of the interface between dyes and nanocrystalline [31–35]. Until now, it remains a severe challenge for both experiment and theory to elucidate the fundamental properties of the ultrafast electron injection [30], and to approach the satisfied efficiency of DSSC. Further developments in dye design will play a crucial part in the ongoing optimization of DSSC [36], and it depends on the quantitative knowledge of dye sensitizer. So the theoretical investigations of the physical properties of dye sensitizers are very important in order to disclose the relationship among the performance, structures and the properties, it is also helpful to design and synthesis novel dye sensitizers with higher performance. Recently a rapid progress of organic dyes has been witnessed reaching close to 10.0% efficiencies in combination with a volatile acetonitrile-based electrolyte [37]. Nitrile is an important class of high performance dyes, which are easily processable, and display good mechanical properties, outstanding thermal and thermal-oxidative stability. Nitrile dyes were used for aerospace, marine,

and electronic packaging applications by thermal treatment of nitrile derivatives at elevated temperatures (generally high up to 350 °C) for an extended period of time. In this paper the performance of 4-Amino-3-Nitrobenzonitrile metal free dye that can be used in DSSC is analyzed.

2. Computational methods

The computations of the geometries, electronic structures, polarizabilities and hyperpolarizabilities, as well as electronic absorption spectrum for dye sensitizer 4-Amino-3-Nitrobenzonitrile was done using *ab initio* HF and DFT with Gaussian03 package [38]. The DFT was treated according to Becke's three parameter gradient-corrected exchange potential and the Lee-Yang-Parr gradient-corrected correlation potential (B3LYP) [39–41], and all calculations were performed without any symmetry constraints by using polarized split-valence 6-311G(d,p) basis sets. The electronic absorption spectrum requires calculation of the allowed excitations and oscillator strengths. These calculations were done using TDDFT with the same basis sets and exchange-correlation functional in vacuum and solution, and the non-equilibrium version of the polarizable continuum model (PCM) [42, 43] was adopted for calculating the solvent effects

3. Results and discussion

3.1. The geometric structure

The optimized geometry of the 4-Amino-3-Nitrobenzonitrile is shown in Fig.1, and the bond lengths, bond angles and dihedral angles are listed in Table 1. Since the crystal structure of the exact title compound is not available till now, the optimized structure can be only be compared with other similar systems for which the crystal structures have been solved. From the theoretical values we can find that most of the optimized bond lengths, bond angles and dihedral angles. The optimized bond lengths of C2-C3 and C4-C5 atoms of 4-Amino-3-Nitrobenzonitrile are 1.38 Å and 1.42 Å respectively at B3LYP/6-311G (d,p) and also well matched with HF/6-311G (d,p).

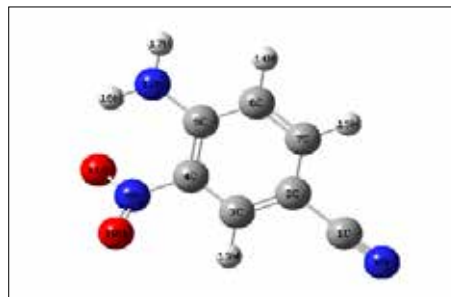


Figure 1. Optimized geometrical structure of dye 4-Amino-3-Nitrobenzonitrile

3.2. Electronic structures and charges

Natural Bond Orbital (NBO) analysis was performed in order to analyze the charge populations of the dye 4-Amino-3-Nitrobenzonitrile. Charge distributions in C, N and H atoms were observed because of the different electro-negativity, the electrons transferred from C atoms to C, N atoms, C atoms to H. The natural charges of different groups are the sum of every atomic natural charge in the group. These data indicate that the cyanine and amide groups are acceptors, while the acetic groups are donors, and the charges were transferred through chemical bonds. The frontier molecular orbital (MO) energies and corresponding density of state of the dye 4-Amino-3-Nitrobenzonitrile is shown in Fig. 2. The HOMO–LUMO gap of the dye 4-Amino-3-Nitrobenzonitrile in vacuum is 5.56 eV.

Table. 1 Bond lengths (in Å), bond angles (in degree) and dihedral angles (in degree) of the dye 4-Amino-3-Nitrobenzonitrile

Parameters	B3LYP/6-11++G(d,p)	HF/6-311++G(d,p)
Bond length(Å)		
C1-C2	1.4274	1.4372
C1-N8	1.156	1.1313
C2-C3	1.3878	1.3716
C2-C7	1.4138	1.4051
C3-C4	1.396	1.3924
C3-H13	1.0808	1.0711
C4-C5	1.4236	1.4081
C4-N9	1.4598	1.4515
C5-C6	1.4204	1.4169
C5-N12	1.3507	1.3427
C6-C7	1.3722	1.3605
C6-H14	1.0843	1.0746
C7-H15	1.0831	1.0746
N9-O10	1.2225	1.1852
N9-O11	1.2386	1.1962
N12-H16	1.0091	0.9907
N12-H17	1.0058	0.9909
Bond Angle(°)		
C1-C2-C3	120.82	120.7568
C1-C2-C7	120.4361	120.4535
C3-C2-C7	118.7439	118.7897
C2-C3-C4	120.7341	120.6989
C2-C3-H13	121.0512	120.7302
C4-C3-H13	118.2147	118.5709
C3-C4-C5	121.4831	121.597
C3-C4-N9	116.6409	116.4489
C5-C4-N9	121.876	121.9542
C4-C5-C6	116.2433	116.1311
C4-C5-N12	124.4558	125.5603
C6-C5-N12	119.3018	118.3086
C5-C6-C7	122.1019	121.9626
C5-C6-H14	118.1319	118.1667
C7-C6-H14	119.7661	119.8707
C2-C7-C6	120.6946	120.8207
C2-C7-H15	119.43997	119.5326
C6-C7-H15	119.8657	119.6467
C4-N9-O10	118.5609	118.1504
C4-N9-O11	118.2267	118.2267
O10-N9-O11	123.2124	123.6229
C5-N12-H16	119.5025	121.0429
C5-N12-H17	119.7927	119.2551
H16-N12-H17	120.7047	119.7014
Dihedral Angle(°)		
C1-C2-C3-C4	179.99	-179.998
C1-C2-C3-H13	-0.0099	0.0038
C7-C2-C3-C4	-0.0074	0.0097
C7-C2-C3-H13	179.9853	180.0014
C1-C2-C7-C6	-179.991	-179.9984
C1-C2-C7-H15	0.0097	0.0009
C3-C2-C7-C6	0.0059	-0.006
C3-C2-C7-H15	-179.9854	179.9933
C2-C3-C4-C5	-0.021	-0.006
C2-C3-C4-N9	-180.0078	-179.9811
H13-C3-C4-C5	-180.0139	-180.0026
H13-C3-C4-N9	-0.0007	0.0171
C3-C4-C5-C6	0.041	-0.011
C3-C4-C5-N12	180.0351	179.9939
N9-C4-C5-C6	-179.9728	179.9681

N9-C4-C5-N12	0.0212	-0.027
C3-C4-N9-O10	-0.0408	-0.0708
C3-C4-N9-O11	179.9811	179.9295
C5-C4-N9-O10	179.9724	179.9491
C5-C4-N9-O11	-0.0057	-0.0506
C4-C5-C6-C7	-0.0348	0.0148
C4-C5-C6-H14	179.9702	180.0093
N12-C5-C6-C7	-180.0291	-179.9898
N12-C5-C6-H14	-0.0241	0.0048
C4-C5-N12-H16	-0.0316	0.1259
C4-C5-N12-H17	180.0762	179.8398
C6-C5-N12-H16	-180.0377	-179.8691
C6-C5-N12-H17	0.0701	-0.1552
C5-C6-C7-C2	0.0082	-0.0066
C5-C6-C7-H15	-179.9925	-180.0059
H14-C6-C7-C2	180.0031	-180.001
H14-C6-C7-H15	-0.0024	-0.00031

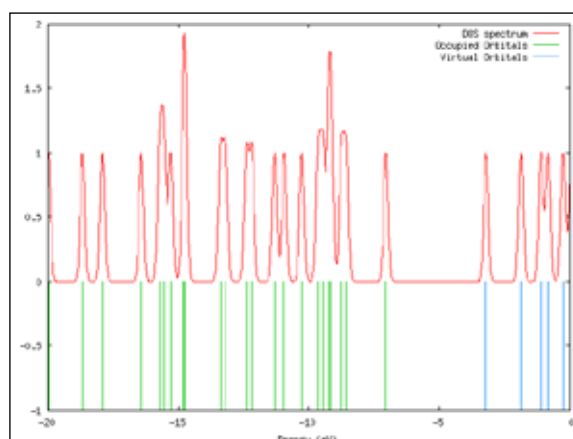


Figure .2. The frontier molecular orbital energies and corresponding density of state (DOS) spectrum of the dye 4-Amino-3-Nitrobenzonitrile

While the calculated HOMO and LUMO energies of the bare Ti38076 cluster as a model for nanocrystalline are -6.55 and -2.77 eV, respectively, resulting in a HOMO–LUMO gap of 3.78 eV, the lowest transition is reduced to 3.20 eV according to TDDFT, and this value is slightly smaller than typical band gap of TiO₂ nanoparticles with nm size [44]. Furthermore, the HOMO, LUMO and HOMO–LUMO gap of (TiO₂)₆₀ clusters is -7.52, -2.97, and 4.55 eV (B3LYP/VDZ), respectively [45]. Taking into account of the cluster size effects and the calculated HOMO, LUMO, HOMO–LUMO gap of the dye 4-Amino-3-Nitrobenzonitrile, Ti38076 and (TiO₂)₆₀ clusters, we can find that the HOMO energies of these dyes fall within the TiO₂ gap.

The above data also reveal the interfacial electron transfer between semiconductor TiO₂ electrode and the dye sensitizer 4-Amino-3-Nitrobenzonitrile is electron injection processes from excited dye to the semiconductor conduction band. This is a kind of typical interfacial electron transfer reaction [46].

3.3. Polarizability and hyperpolarizability

Polarizabilities and hyperpolarizabilities characterize the response of a system in an applied electric field [47]. They determine not only the strength of molecular interactions (long-range intermolecular induction, dispersion forces, etc.) as well as the cross sections of different scattering and collision processes, but also the nonlinear optical properties (NLO) of the system [48, 49]. It has been found that the dye sensitizer hemicyanine system, which has high NLO property, usually possesses high photoelectric conversion performance [50]. In order to investigate the relationships among photocurrent generation, molecular structures and NLO, the polarizabilities and hyperpolarizabilities of 4-Amino-3-Nitrobenzonitrile was calculated.

The polarizabilities and hyperpolarizabilities could be computed via finite field (FF) method, sum-over state (SOS) method based on TD-DFT, and coupled-perturbed HF (CPHF) method. However, the use of FF, SOS, and CPHF methods with large sized basis sets for 4-Amino-

3-Nitrobenzonitrile is too expensive. Here, the polarizability and the first hyperpolarizabilities are computed as a numerical derivative of the dipole moment using B3LYP/6-31G (d,p). The definitions [48, 49] for the isotropic polarizability $\alpha = \frac{1}{3}(\alpha_{xx} + \alpha_{yy} + \alpha_{zz})$

The polarizability anisotropy invariant is

$$\Delta\alpha = \left[\frac{(\alpha_{xx} - \alpha_{yy})^2 + (\alpha_{yy} - \alpha_{zz})^2 + (\alpha_{zz} - \alpha_{xx})^2}{2} \right]^{1/2}$$

and the average hyperpolarizability is

$$\beta_{||} = \frac{1}{5}(\beta_{iiz} + \beta_{izi} + \beta_{zii})$$

Where, α_{xx} , α_{yy} , and α_{zz} are tensor components of polarizability; β_{iiz} , β_{izi} , and β_{zii} (i from X to Z) are tensor components of hyperpolarizability.

Table 2 Polarizability (α) of the dye 4-Amino-3-Nitrobenzonitrile (in a.u.).

α_{xx}	α_{xy}	α_{yy}	α_{xz}	α_{yz}	α_{zz}	α	$\Delta\alpha$
-91.1292	2.7424	-63.0324	-0.0913	0.0800	-69.9985	74.73	17.92

Table 3 Hyperpolarizability (β) of the dye 4-Amino-3-Nitrobenzonitrile (in a.u.).

β_{xxx}	β_{xxy}	β_{xyy}	β_{yyy}	β_{xxz}	β_{xyz}	β_{yyz}	β_{xzz}	β_{yzz}	β_{zzz}	β_{ii}
119.22	59.07	12.68	42.59	1.39	0.10	0.73	0.107	-7.53	-0.59	1.63

Tables 2 and 3 list the values of the polarizabilities and hyperpolarizabilities of the dye 4-Amino-3-Nitrobenzonitrile. In addition to the individual tensor components of the polarizabilities and the first hyperpolarizabilities, the isotropic polarizability, polarizability anisotropy invariant and hyperpolarizability are also calculated. The calculated isotropic polarizability of 4-Amino-3-Nitrobenzonitrile 74.73 a.u. However, the calculated isotropic polarizability of JK16, JK17, dye 1, dye 2, D5, DST and DSS is 759.9, 1015.5, 694.7, 785.7, 510.6, 611.2 and 802.9 a.u., respectively [51,52]. The above data indicate that the donor-conjugate p bridge-acceptor (D-p-A) chain-like dyes have stronger response for external electric field. Whereas, for dye sensitizers D5, DST, DSS, JK16, JK17, dye 1 and dye 2, on the basis of the published photo-to-current conversion efficiencies, the similarity and the difference of geometries, and the calculated isotropic polarizabilities, it is found that the longer the length of the conjugate bridge in similar dyes, the larger the polarizability of the dye molecule, and the lower the photo-to-current conversion efficiency. This may be due to the fact that the longer conjugate p-bridge enlarged the delocalization of electrons, thus it enhanced the response of the external field, but the enlarged delocalization may be not favorable to generate charge separated state effectively. So it induces the lower photo-to-current conversion efficiency.

3.4. Electronic absorption spectra and sensitized mechanism

In order to understand the electronic transitions of 4-Amino-3-Nitrobenzonitrile, TD-DFT calculations on electronic absorption spectra in vacuum and solvent were performed, and the results are shown in Fig. 3. It is observed that, for 4-Amino-3-Nitrobenzonitrile, the absorption in the visible region is much weaker than that in the UV region. The calculated results have a red-shift. The results of TD-DFT have an appreciable red-shift, and the degree of red-shift in solvent is more significant than that in vacuum. The discrepancy between vacuum and solvent effects in TD-DFT calculations may result from two aspects. The first aspect is smaller gap of materials which induces smaller excited energies. The other is solvent effects. Measurements of electronic absorptions are usually performed in Solvent, especially polar solvent, could affect the geometry and electronic structure as well as the properties of molecules through the long-range interaction between solute molecule and solvent molecule. For these reasons it is more difficult to make the TD-DFT calculation is consistent with quantitatively. Though the discrepancy exists, the TD-DFT calculations are capable of describing the spectral features of 4-Amino-3-Nitrobenzonitrile because of the agreement of lineshape and relative strength as compared with the vacuum and solvent.

The HOMO-LUMO gap of 4-Amino-3-Nitrobenzonitrile in acetonitrile at B3LYP/6-31G (d,p) theory level is smaller than that in vacuum. This

fact indicates that the solvent effects stabilize the frontier orbitals of 4-Amino-3-Nitrobenzonitrile. So it induces the smaller intensities and red-shift of the absorption as compared with that in vacuum.

In order to obtain the microscopic information about the electronic transitions, the corresponding MO properties are checked. The absorption in visible and near-UV region is the most important region for photo-to-current conversion, so only the 20 lowest singlet/singlet transitions of the absorption band in visible and near-UV region for 4-Amino-3-Nitrobenzonitrile is listed in Table 4. The data of Table 4 and Fig. 4 are based on the 6-311G (d,p) results with solvent effects involved.

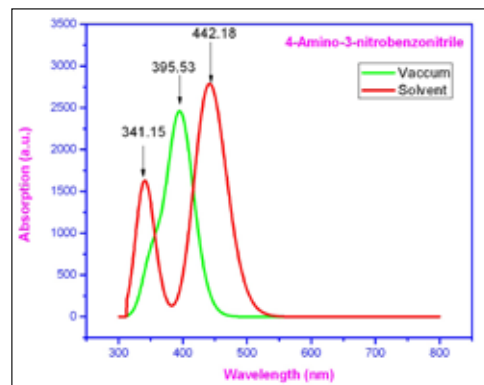


Figure .3. Calculated electronic absorption spectra of the dye 4-Amino-3-Nitrobenzonitrile.

This indicates that the transitions are photo induced charge transfer processes, thus the excitations generate charge separated states, which should favour the electron injection from the excited dye to semiconductor surface.

The solar energy to electricity conversion efficiency (η) under AM 1.5 white-light irradiation can be obtained from the following formula:

$$\eta(\%) = \frac{J_{sc}[mAcm^{-2}]V_{oc}[V]ff}{I_0[mWcm^{-2}]} \times 100$$







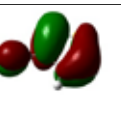
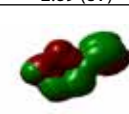
HOMO-3		LUMO+3	
	-10.28 (eV)		-0.29 (eV)
HOMO-2		LUMO+2	
	-9.26 (eV)		-1.106 (eV)
HOMO-1		LUMO+1	
	-9.29 (eV)		-2.89 (eV)
HOMO		LUMO	
	-8.78 (eV)		-3.22 (eV)

Figure .4. Isodensity plots (isodensity contour = 0.02 a.u.) of the frontier orbitals of 4-Amino-3-Nitrobenzonitrile

Where I_0 is the photon flux, J_{sc} is the short-circuit photocurrent density, and V_{oc} is the open-circuit photovoltage, and ff represents the fill factor [53]. At present, the J_{sc} , the V_{oc} , and the ff are only obtained by experiment, the relationship among these quantities and the electronic structure of dye is still unknown. The analytical relationship between V_{oc} and ELUMO may exist. According to the sensitized mechanism (electron injected from the excited dyes to the semiconductor conduction band) and single electron and single state approximation, there is an energy relationship:

Table 4 Computed excitation energies, electronic transition configurations and oscillator strengths (f) for the optical transitions with $f > 0.01$ of the absorption bands in visible and near-UV region for the dye 4-Amino-3-Nitrobenzonitrile in acetonitrile.

State	Configurations composition (corresponding transition orbitals)	Excitation energy (eV/nm)	oscillator strength (f)
1	-0.11422 (40 → 43) 0.66348 (42 → 43)	3.2354/383.22	0.1736
2	-0.19643 (39 → 43) 0.64433 (40 → 43)	3.6279/341.75	0.0102
3	-0.40308 (41 → 43) 0.57400 (42 → 44)	4.0847/303.53	0.0018
4	-0.13068 (39 → 44) 0.54484 (41 → 43) 0.38388 (42 → 44)	4.2965/288.57	0.0407
5	0.67671 (37 → 43)	4.6629/265.90	0.0023
6	0.62581 (39 → 43) 0.18544 (40 → 43) 0.10230 (42 → 45)	4.7976/ 258.43	0.1797
7	-0.11683 (41 → 44) 0.66930 (42 → 45)	5.3675/ 230.99	0.0056
8	0.53978 (38 → 43) -0.23462 (39 → 44) -0.21208 (40 → 44) 0.11172 (41 → 44)	5.6747/ 218.48	0.0444
9	0.17949 (38 → 43) -0.10102 (39 → 44) 0.66002 (40 → 44)	5.7753/214.68	0.0169
10	-0.25332 (39 → 44) 0.59300 (42 → 46) 0.16491 (42 → 47) 0.11605 (42 → 48)	5.8779/ 210.93	0.0079
11	-0.19934 (38 → 43) -0.27367 (39 → 44) -0.12084 (39 → 45) 0.48237 (41 → 44) -0.22193 (41 → 45) -0.12342 (42 → 46)	5.8861/ 210.64	0.2558
12	0.43701 (39 → 44) 0.36097 (41 → 44) 0.18882 (41 → 45) 0.26091 (42 → 46)	5.9701/ 207.67	0.3456
13	-0.14555 (42 → 46) 0.66967 (42 → 47) -0.12264 (42 → 48)	6.2555/198.20	0.0249
14	0.15520 (33 → 43) -0.30583 (34 → 43) 0.60426 (36 → 43)	6.3612/ 194.91	0.0010
15	0.13627 (35 → 43) 0.63655 (38 → 44) 0.19102 (42 → 48)	6.4833/ 191.23	0.0019
16	-0.21212 (38 → 44) -0.17297 (42 → 46) 0.60085 (42 → 48) 0.17816 (42 → 49)	6.4990/ 190.77	0.0024
17	-0.18347 (33 → 43) 0.53990 (34 → 43) 0.19248 (35 → 43) 0.34089 (36 → 43)	6.5647/188.87	0.0225
18	-0.20389 (34 → 43) 0.64141 (35 → 43) -0.11201 (38 → 44)	6.6493/186.46	0.0077
19	-0.20206 (42 → 48) 0.65829 (42 → 49)	6.7091/ 184.80	0.0083
20	0.67637 (37 → 44) -0.14058 (40 → 45)	6.7637 /183.31	0.0005

$$eV_{oc} = E_{LUMO} - E_{CB}$$

Where, E_{CB} is the energy of the semiconductor's conduction band edge. So the V_{oc} may be obtained applying the following formula:

$$V_{oc} = \frac{(E_{LUMO} - E_{CB})}{e}$$

It induces that the higher the ELUMO, the larger the V_{oc} . The results of organic dye sensitizer JK16 and JK17 [39], D-ST and D-SS also proved the tendency [54] (JK16: LUMO = -2.73 eV, V_{oc} = 0.74 V; JK17: LUMO = -2.87 eV, V_{oc} = 0.67 V; D-SS: LUMO = -2.91 eV, V_{oc} = 0.70 V; D-ST: LUMO = -2.83 eV, V_{oc} = 0.73 V). Certainly, this formula expects further test by experiment and theoretical calculation. The J_{sc} is determined by two processes, one is the rate of electron injection from the excited dyes to the conduction band of semiconductor, and the other is the rate of redox between the excited dyes and electrolyte. Electrolyte effect on the redox processes is very complex, and it is not taken into account in the present calculations. This indicates that most of excited states of 4-Amino-3-Nitrobenzonitrile have larger absorption coefficient, and then with shorter lifetime for the excited states, so it results in the higher electron injection rate which leads to the larger J_{sc} of 4-Amino-3-Nitrobenzonitrile. On the basis of above analysis, it is clear that the 4-Amino-3-Nitrobenzonitrile has better performance in DSSC.

4. Conclusions

The geometries, electronic structures, polarizabilities, and hyperpolarizabilities of dye 4-Amino-3-Nitrobenzonitrile was studied by using ab initio HF and density functional theory with hybrid functional B3LYP,

and the UV-Vis spectra were investigated by using TD-DFT methods. The NBO results suggest that 4-Amino-3-Nitrobenzonitrile is a (D-p-A) system. The calculated isotropic polarizability of 4-Amino-3-Nitrobenzonitrile is 74.73 a.u. The calculated polarizability anisotropy invariant of 4-Amino-3-Nitrobenzonitrile is 17.92 a.u. The hyperpolarizability of 4-Amino-3-Nitrobenzonitrile is 1.63 a.u. The electronic absorption spectral features in visible and near-UV region were assigned based on the qualitative agreement to TD-DFT calculations. The absorptions are all ascribed to $\pi \rightarrow \pi^*$ transition. The three excited states with the lowest excited energies of 4-Amino-3-Nitrobenzonitrile is photoinduced electron transfer processes that contributes sensitization of photo-to-current conversion processes. The interfacial electron transfer between semiconductor TiO₂ electrode and dye sensitizer 4-Amino-3-Nitrobenzonitrile is electron injection process from excited dye as donor to the semiconductor conduction band. Based on the analysis of geometries, electronic structures, and spectrum properties between 4-Amino-3-Nitrobenzonitrile the role of nitro group is as follows: it enlarged the distance between electron donor group and semiconductor surface, and decreased the timescale of the electron injection rate, resulted in giving lower conversion efficiency. This indicates that the choice of the appropriate conjugate bridge in dye sensitizer is very important to improve the performance of DSSC.

Acknowledgement:

This work was partly financially supported by University Grants Commission, Govt. of India, New Delhi, within the Major Research Project scheme under the approval-cum-sanction No. F.No.34-5\2008(SR) & 34-1/TN/08.

REFERENCES

- [1] B. Li, L. Wang, B. Kang, P. Wang, Y. Qiu, *Sol. Energy Mater. Sol. Cells* 90 (2006) 549. [2] B. O'Regan, M. Gratzel, *Nature* 353 (1991) 737. [3] M. Gratzel, *J. Photochem. Photobiol. C* 4 (2003) 145. [4] M. Gratzel, *J. Photochem. Photobiol. A* 164 (2004) 3. [5] M.K. Nazeeruddin, C. Klein, P. Liska, M. Gratzel, *Coord. Chem. Rev.* 249 (2005) 1460. [6] T. Dittrich, B. Neumann, H. Tributsch, *J. Phys. Chem. C* 111 (2007) 2265. [7] X.Z. Liu, Y.H. Luo, H. Li, Y.Z. Fan, Z.X. Yu, Y. Lin, L.Q. Chen, Q.B. Meng, *Chem. | Commun.* 27 (2007) 2847. [8] J.B. Xia, F.Y. Li, H. Yang, X.H. Li, C.H. Huang, *J. Mater. Sci.* 42 (2007) 6412. [9] M.X. Li, X.B. Zhou, H. Xia, H.X. Zhang, Q.J. Pan, T. Liu, H.G. Fu, C.C. Sun, *Inorg. Chem.* 47 (2008) 2312. [10] E. Muller, P. Liska, N. Vlachopoulos, M. Gratzel, *J. Am. Chem. Soc.* 115 (1993) 6382. [11] M.K. Nazeeruddin, P. Pechy, T. Renouard, S.M. Zakeeruddin, R. Humphry-Baker, P. Comte, P. Liska, L. Cevey, E. Costa, V. Shklover, L. Spiccia, G.B. Deacon, C.A. Bignozzi, | M. Gratzel, *J. Am. Chem. Soc.* 123 (2001) 1613. [12] M. Gratzel, *Inorg. Chem.* 44 (2005) 6841. [13] K. Hara, T. Sato, R. Katoh, A. Furube, Y. Ohga, A. Shinpo, S. Suga, K. Sayama, | H. Sugihara, H. Arakawa, *J. Phys. Chem. B* 107 (2003) 597. [14] X.H. Zhang, C. Li, W.B. Wang, X.X. Cheng, X.S. Wang, B.W. Zhang, *J. Mater. Chem.* 17 | (2007) 642 (and reference therein). [15] M. Liang, W. Xu, F. Cai, P. Chen, B. Peng, J. Chen, Z. Li, *J. Phys. Chem. C* 111 (2007) | 4465 (and reference therein). [16] W. Xu, B. Peng, J. Chen, M. Liang, F. Cai, *J. Phys. Chem. C* 112 (2008) 874. [17] F. De Angelis, S. Fantacci, A. Selloni, *Chem. Phys. Lett.* 389 (2004) 204. [18] F. De Angelis, S. Fantacci, A. Selloni, M.K. Nazeeruddin, *Chem. Phys. Lett.* 415 (2005) 115. [19] Y. Xu, W.K. Chen, M.J. Cao, S.H. Liu, J.Q. Li, A.I. Philippopoulos, P. Falaras, *Chem. | Phys.* 330 (2006) 204. [20] M.K. Nazeeruddin, F. De Angelis, S. Fantacci, A. Selloni, G. Viscardi, P. Liska, S. | Ito, B. Takeru, M. Gratzel, *J. Am. Chem. Soc.* 127 (2005) 16835. [21] F. De Angelis, S. Fantacci, A. Selloni, M. Gratzel, M.K. Nazeeruddin, *Nano. Lett.* | 10 (2007) 3189. [22] F. De Angelis, S. Fantacci, A. Selloni, M.K. Nazeeruddin, M. Gratzel, *J. Am. Chem. | Soc.* 129 (2007) 14156. [23] F. De Angelis, S. Fantacci, A. Selloni, *Nanotechnology* 19 (2008) 424002. [24] D. Di Censo, S. Fantacci, F. De Angelis, C. Klein, N. Evans, K. Kalyanasundaram, | H.J. Bolink, M. Gratzel, M.K. Nazeeruddin, *Inorg. Chem.* 47 (2008) 980. [25] Y. Kurashige, T. Nakajima, S. Kurashige, K. Hirao, Y. Nishikitani, *J. Phys. Chem. A* | 111 (2007) 5544. [26] M.P. Balanay, D.H. Kim, *Phys. Chem. Chem. Phys.* 10 (2008) 5121. [27] P. Persson, M.J. Lundqvist, *J. Phys. Chem. B* 109 (2005) 11918. [28] P. Persson, M.J. Lundqvist, R. Ernstorfer, W.A. Goddard III, F. Willig, *J. Chem. | Theory Comput.* 2 (2006) 441. [29] M.J. Lundqvist, M. Nisling, S. Lunell, B. Akemark, P. Persson, *J. Phys. Chem. B* | 110 (2006) 20513. [30] M. Nisling, P. Persson, S. Lunell, L. Ojamae, *J. Phys. Chem. C* 111 (2007) 12116. [31] W.R. Duncan, O.V. Prezhdo, *Annu. Rev. Phys. Chem.* 58 (2007) 143. [32] W.R. Duncan, O.V. Prezhdo, *J. Am. Chem. Soc.* 130 (2008) 9756. [33] L.G.C. Rego, V.S. Batista, *J. Am. Chem. Soc.* 125 (2003) 7989. [34] Z.Y. Guo, Y. Zhao, W.Z. Liang, G.H. Chen, *J. Phys. Chem. C* 112 (2008) 16655. [35] I. Kondov, M. Clizek, C. Benesch, H.B. Wang, M. Thoss, *J. Phys. Chem. C* 111 (2007) | 11970. [36] N. Robertson, *Angew. Chem. Int. Ed.* 45 (2006) 2338. [37] S. Ito, H. Miura, S. Uchida, K. Takata, K. Sumioka, P. Liska, P. Comte, P. Pechy, M. | Gratzel, *Chem. Commun.* (2008), 5194-5196. [38] M.J. Frisch, G.W. Trucks, H.B. Schlegel, G.E. Scuseria, M.A. Robb, J.R. Cheeseman, J.A. | Montgomery Jr., T. Vreven, K.N. Kudin, J.C. Burant, J.M. Millam, S.S. Iyengar, J. Tomasi, | V. Barone, B. Mennucci, M. Cossi, G. Scalmani, N. Rega, G.A. Petersson, H. Nakatsuji, M. | Hada, M. Ehara, K. Toyota, R. Fukuda, J. Hasegawa, M. Ishida, T. Nakajima, Y. Honda, O. | Kitao, H. Nakai, M. Klene, X. Li, J.E. Knox, H.P. Hratchian, J.B. Cross, C. Adamo, J. | Jaramillo, R. Gomperts, R.E. Stratmann, O. Yazyev, A.J. Austin, R. Cammi, C. Pomelli, J.W. | Ochterski, P.Y. Ayala, K. Morokuma, G.A. Voth, P. Salvador, J.J. Dannenberg, V.G. | Zakrzewski, S. Dapprich, A.D. Daniels, M.C. Strain, O. Farkas, D.K. Malick, A.D. Rabuck, K. | Raghavachari, J.B. Foresman, J.V. Ortiz, Q. Cui, A.G. Baboul, S. Clifford, J. Cioslowski, B.B. | Stefanov, G. Liu, A. Liashenko, P. Piskorz, I. Komaromi, R.L. Martin, D.J. Fox, T. Keith, | M.A. Al-Laham, C.Y. Peng, A. Nanayakkara, M. Challacombe, P.M.W. Gill, B. Johnson, W. | Chen, M.W. Wong, C. Gonzalez, J.A. Pople, Gaussian 03, Gaussian, Inc., Pittsburgh, PA, | 2003. [39] A.D. Becke, *J. Chem. Phys.* 98 (1993), 5648-5652. [40] B. Miehlich, A. Savin, H. Stoll, H. Preuss, *Chem. Phys. Lett.* 157 (1989), 200-206. [41] C. Lee, W. Yang, R.G. Parr, *Phys. Rev. B* 37 (1988), 785-789. [42] V. Barone, M. Cossi, *J. Phys. Chem. A* 102 (1998), 1995-2001. [43] M. Cossi, N. Rega, G. Scalmani, V. Barone, *J. Comput. Chem.* 24 (2003), 669-681. [44] M.K. Nazeeruddin, F. De Angelis, S. Fantacci, A. Selloni, G. Viscardi, P. Liska, S. Ito, B. | Takeru, M. Gratzel, *J. Am. Chem. Soc.* 127 (2005), 16835-16847. [45] M.J. Lundqvist, M. Nisling, P. Persson, S. Lunell, *Int. J. Quantum Chem.* 106 (2006), 3214 | 3234. [46] D.F. Waston, G.J. Meyer, *Annu. Rev. Phys. Chem.* 56 (2005), 119-156. [47] C. R. Zhang, H. S. Chen, and G. H. Wang, *Chem. Res. Chin. U.* 20 (2004), 640-646. [48] Y. Sun, X. Chen, L. Sun, X. Guo, W. Lu, *Chem. Phys. Lett.* 381 (2003), 397-403. [49] O. Christiansen, J. Gauss, J. F. Stanton, *Chem. Phys. Lett.* 305 (1999), 147-155. [50] Z. S. Wang, Y. Y. Huang, C. H. Huang, J. Zheng, H.M. Cheng, S. J. Tian, *Synth. Met.* 14 | (2000), 201-207. [51] C.R. Zhang, Y.Z. Wu, Y.H. Chen, H.S. Chen, *Acta Phys. Chim. Sin.* 25 (2009), 53-60. [52] A. Seidl, A. Gorling, P. Vogl, J. A. Majewski, M. Levy, *Phys. Rev. B* 53 (1996), 3764 | 3774. [53] K. Hara, T. Sato, R. Katoh, A. Furube, Y. Ohga, A. Shinpo, S. Suga, K. Sayama, | H. Sugihara, H. Arakawa, *J. Phys. Chem. B.* 107 (2003), 597-606. [54] C.R. Zhang, Z.J. Liu, Y.H. Chen, H.S. Chen, Y.Z. Wu, L.H. Yuan, *J. Mol. Struct. | (THEOCHEM)* 899 (2009), 86-93. |